The Flow of Excitation Energy in LHCII Monomers: Implications for the Structural Model of the Major Plant Antenna

Claudiu C. Gradinaru,* Sevgi Özdemir,# Demet Gülen,# Ivo H.M. van Stokkum,* Rienk van Grondelle,* and Herbert van Amerongen*

*Department of Physics and Astronomy and Institute for Condensed Matter and Optical Physics, Free University of Amsterdam, De Boelelaan 1081, 1081 HV Amsterdam, The Netherlands, and #Physics Department, Middle East Technical University, Ankara 06531, Turkey

ABSTRACT Spectral and kinetic information on energy transfer within the light-harvesting complex II (LHCII) monomer was obtained from this subpicosecond transient absorption study, by using selective excitation (663, 669, 672, 678, and 682 nm) of various Chl *a* absorption bands and detecting the induced changes over the entire Q_y region (650–700 nm). It is shown that transfer from the pigment(s) absorbing around 663 nm to the low energy ones occurs in 5 ± 1 ps, whereas the 670-nm excitation is delivered to the same "destination" in two phases (0.30 ± 0.05 ps, and 12 ± 2 ps), and a fast equilibration (lifetime 0.45 ± 0.05 ps) takes place within the main absorption band (675–680 nm). From comparison with results from similar time-resolved measurements on trimeric samples, it can be concluded that the intramonomeric energy transfer completely determines the spectral equilibration observed in native LHCII complexes. To correlate the measured lifetimes and their associated spectra with the pigment organization within the available structural model of LHCII (Kühlbrandt et al. 1994. *Nature.* 367:614–621), extensive but straightforward theoretical modeling was used. Thus it is demonstrated that the pigment assignment (Chl *a* or Chl *b*) given by Kühlbrandt and co-workers cannot simultaneously describe the dichroic spectra and the transient absorption results for the rather homologous LHCII and CP29 proteins. A more recent assignment for CP29, in which a Chl *b* molecule ("Chl *b*5") is identified as a Chl *a* (Dr. R. Bassi, personal communication), leads to a much better description of both CP29 and LHCII. Furthermore, the orientations of the transition dipole moments, which have not been obtained in the crystal structure, are now assigned for most of the Chl's.

INTRODUCTION

Photosynthetic organisms possess the ability to convert solar energy into chemical energy (stored in the form of ATP and NADPH), which is further used to drive their metabolism. Light harvesting is the first step in photosynthesis and is mainly performed by a set of antenna complexes, i.e., transmembrane proteins binding light-absorbing molecules such as chlorophylls (Chl's) and carotenoids (Car's) (see, e.g., van Grondelle et al., 1994). Containing about half of the Chl's active in plant photosynthesis, light-harvesting complex II (LHCII) is one of the most thoroughly investigated antennae. It is known that LHCII is a trimeric complex that usually transfers excited-state energy toward the reaction center core of photosystem II (PSII), where a sequence of electron transfer reactions leads to the conversion into chemical energy. Chemical analysis (high-performance liquid chromatography, HPLC) has shown that each monomeric subunit of LHCII binds five or six Chl *b*, seven or eight Chl *a*, and several Car molecules: two luteins, one neoxanthin, and varying, substoichiometric amounts of violaxanthin (see, e.g., Peterman et al., 1997a).

Based on electron crystallography on two-dimensional crystals, a structural model of LHCII was proposed (Kühlbrandt et al., 1994). The resolution achieved (3.4 Å) allowed the identification, in each monomer, of two central carotenoids (assumed to be luteins) surrounded by 12 Chl molecules. However, a clear distinction between Chl *a* and Chl *b*, or between Q_x and Q_y directions within single chlorophylls, could not be made. The shortest interpigment distances range from 4 to 5 Å between tetrapyrrole rings of nearest-neighbor Chl's and between the luteins and closest Chl's. Based on this proximity and on the observed ultrafast transfer of excitation from Chl *b* to Chl *a*, an assignment was put forward by Kühlbrandt et al. (1994), in which the closest Chl pairs are Chl *b*–Chl *a* couples and the seven Chl's closest to the luteins are Chl *a*, to enable efficient triplet quenching. Although reasonable, this assignment might not be entirely correct, because it was shown that lutein is not the only carotenoid species involved in quenching triplets in LHCII (van der Vos et al., 1991; Peterman et al., 1995). The assignment of the Chl's in LHCII was challenged by Connelly et al. (1997a), based on a pump-probe study aiming at the detection of Car-to-Chl singlet energy transfer. However, the conclusion from this study that two Chl *b* are in close contact with the central Car's was in disagreement with a study by Peterman et al. (1997b), in which no evidence for such connections was found.

LHCII in the trimeric form has been studied extensively with both steady-state and time-resolved spectroscopy. The existence of 9–11 Chl Q_y bands in a relatively small spectral domain (630–690 nm) has been revealed by (polarized) absorption and Stark spectroscopy (Hemelrijk et al., 1992; Krawczyk et al., 1993; Nussberger et al., 1994). The excited-

Received for publication 13 April 1998 and in final form 23 July 1998.

Address reprint requests to Dr. Claudiu C. Gradinaru, Department of Physics and Astronomy, Free University of Amsterdam, De Boelelaan 1081, 1081 HV, Amsterdam, The Netherlands. Tel.: 31-20-444-7942; Fax: 31-20-444-7899; E-mail: klaus@nat.vu.nl.

0006-3495/98/12/3064/14 $2.00

state kinetics, investigated with various time-resolved techniques, is characterised by ultrafast Chl *b*-to-Chl *a* transfer occurring with at least three distinct lifetimes ($\lesssim$200 fs, ~600 fs, and 2–6 ps), energy redistribution among the Chl *a* spectral pools with time constants of $\lesssim$300 fs, 2–4 ps and 10–20 ps, and a slow relaxation (2–4 ns) of the equilibrated state (Mullineaux et al., 1993; Bittner et al., 1994; Visser et al., 1996; Connelly et al., 1997b). In a recent work by Trinkunas et al. (1997) a model for the spectra and the orientation of all Chl molecules was obtained, which satisfactorily (but by no means uniquely) reproduces the steady-state as well as the room temperature transient absorption data. Partly guided by the work of Connelly et al. (1997a), it suggested a swap of two Chl *a* with Chl *b* locations as compared to the Chl identities proposed by Kühlbrandt and co-workers (1994).

By using subpicosecond transient absorption spectroscopy on LHCII monomers, excitation energy transfer (EET) from Chl *b* to Chl *a* was recently found to have an entirely intramonomeric character (Kleima et al., 1997). Using the same sample and experimental technique, we address here questions concerning the nature (inter- or intramonomeric) of the excitation energy transfer (EET) steps involving only the Chl *a* pigments. Upon selective excitation of various Chl *a* bands, which is possibly due to sharpening of the absorption bands at 77 K, detailed information can be obtained about spectral equilibration within one monomeric subunit of the trimer. It is shown, by applying a straightforward modeling approach and by combining results from both polarized and femtosecond spectroscopy, that considerable progress can be achieved in elucidating the orientation and the spectral properties of each pigment in the LHCII structure. The results do not support the conclusions of the model mentioned above (Trinkunas et al., 1997) about the assignment of the Chl *a* and Chl *b* identities, but are in line with an assignment for the homologous protein CP29 (Dr. R. Bassi, personal communication).

MATERIALS AND METHODS

Sample preparation

Trimeric LHCII was prepared starting with BBY membrane fragments from spinach, using a method described earlier (Peterman et al., 1995). The monomeric subunits were obtained from trimers by incubation with 1% (w/v) octyl glucoside and 10 μg/ml phospholipase A_2 (Peterman et al., 1997a). Free pigments and some remaining trimers were removed by sucrose gradient (5–20% w/v) centrifugation (overnight at 200 $\times$ *g*). Further removal of the unbound pigments was achieved with a Mono-Q anion-exchange fast protein liquid chromatography column (Pharmacia). For the pump-probe experiments, the monomers were solubilized in a buffer containing 0.06% (w/v) n-dodecyl β,D-maltoside, 80% (v/v) glycerol, and 20 mM HEPES (pH 7.5). All measurements were performed at 77 K in a liquid nitrogen cryostat (DN1704; Oxford Instruments). The optical density at 677.5 nm was ~0.6 in cuvettes with a 2-mm pathlength.

Laser system

Transient absorption data were recorded with subpicosecond time resolution on a spectrophotometer described elsewhere (Visser et al., 1995). A low repetition rate (30 Hz) ensured the absence of accumulating Chl *a* triplet states at 77 K. Excitation pulses between 663 and 682 nm were selected from the white light continuum with interference filters (6–7 nm full width at half-maximum) and then amplified in a single dye cell (4-dicyanomethylene-2-methyl-6-p-dimethylaminostyryl-4H-pyran). The probing light was generated in a sapphire plate, divided into a probe and a reference beam, and projected onto two separate diode arrays. Both beams were polarized under the magic angle (54°45′) relative to the vertically polarized pump beam. The pump pulses, with energies of 0.1–0.4 μJ, were focused on a spot of ~0.3 mm diameter in the sample, resulting in excitation densities $\lesssim 10^{15}$ photons/pulse/cm^2. Transient difference spectra were measured for 38 delays between pump and probe pulses, up to 600 ps. One data set was the result of averaging more than 300 shots for each delay position, and at least four data sets were recorded for each pump wavelength. The spectra were detected with 0.5-nm resolution over a wavelength window spanning a range from 640 to 700 nm. The maximum changes in absorption in these experiments were around 100 mOD, with a noise level of less than 5 mOD. Absorption spectra of the LHCII sample taken before and after the measurements proved to be identical.

Data analysis

The time-gated spectra were analyzed with a global fitting routine as described previously (van Stokkum et al., 1994). Data sets for the same excitation wavelength were fitted together in an irreversible sequential model with increasing lifetimes, to yield species-associated difference spectra (SADS) and characteristic decay times. The instrument response function, fitted with a Gaussian profile, had FWHM values of 200–250 fs. Thus the main imprecision occurred in determining the fastest lifetime(s), a factor that is included in the error margins of the results given below.

RESULTS

The 77 K absorption spectrum of the monomeric LHCII samples used for pump-probe spectroscopy is shown in Fig. 1. For comparison, the spectrum of the trimers measured under similar conditions is given in the same picture. The major differences are located in the Chl *a* Q_y region and consist of the decrease plus the red shift from 675 nm to 677.5 nm of the absorption maximum, and, concomitantly, the change of the 670-nm shoulder into a distinct peak for monomers. In addition, minor differences are observed around 665 nm and in the Chl *b* absorption, near 645 nm. HPLC analysis (Peterman et al., 1997a) indicated that these

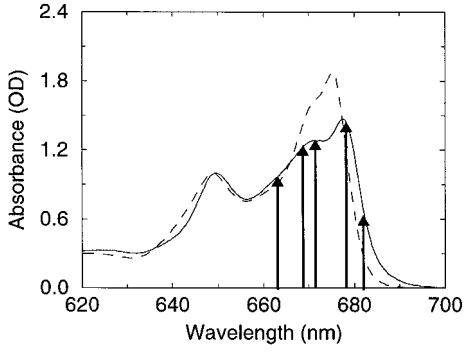

FIGURE 1 77 K absorption spectra of LHC-II monomers (*solid line*) and trimers (*dashed line*), recorded with a 0.5-nm bandwidth. The arrows indicate the excitation wavelengths used in this study: 663, 669, 671.5, 678, and 682 nm.

monomers each contain six Chl *b* and almost seven Chl *a*, approximately one Chl *a* molecule less than in the monomeric subunits of the intact trimers. In this transient absorption study different Chl *a* pools were selectively populated by excitation pulses whose center wavelengths (663, 669, 672, 678, and 682 nm) are indicated by arrows in Fig. 1.

Fig. 2 shows difference absorption spectra measured for various delays between the pump and the probe pulses where the pump pulse was centered at 663 nm. In the first spectrum (*solid line*), which approximates the time zero signal, bleaching/stimulated emission (SE) appears not only around the excitation wavelength but also around 670 and 677 nm, most probably because of direct excitation of the corresponding pools via the vibronic side bands. However, ultrafast energy transfer processes between different electronic states cannot be ruled out a priori (but see below). The next difference spectrum (*dashed line*), recorded at a delay of 2.5 ps, exhibits a significant increase in the signal above 674 nm plus a small red shift of the maximum from 677 to 678 nm, in parallel with the decrease observed at shorter wavelengths. It takes several picoseconds for the bleaching/SE around 663 nm to disappear and even longer for the signal in the 670-nm region, whereas at later times (tens and hundreds of picoseconds) the major process is the decay of the spectrally equilibrated state.

Global analysis of these data in the 640–690-nm spectral range with an irreversible sequential model A $\rightarrow$ B$\rightarrow$ C $\rightarrow$ D $\rightarrow \cdots$ was justified by the absence of uphill energy transfer at 77 K, where the Boltzmann factor kT is equal to 2.5–3 nm. This means that state A, formed by the excitation pulse within the instrument response time, decays with a time constant τ_A into state B, which decays into state C with a longer time constant τ_B, and so on, until the system relaxes back to the ground state. For the present case, the minimum number of lifetimes necessary for a satisfactory description of the spectral evolution was four: 120 fs, 7.5 ps, 135 ps, and 3.4 ns (fluorescence lifetime of Chl *a* in solution, a fixed but relatively unimportant parameter in the fitting program). The spectra corresponding to each of the intermediate states (SADS) are presented in Fig. 3, *A–D.*

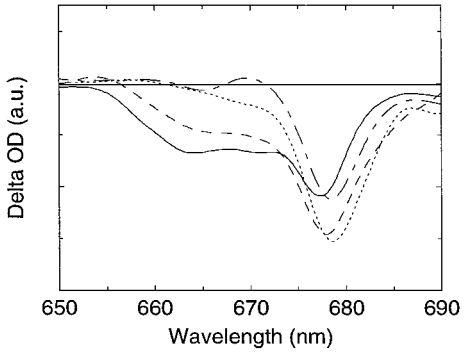

FIGURE 2 Transient absorption difference spectra measured after 663-nm excitation, at four delay times between the pump and the probe pulses: $t \approx 0$ (*solid line*), 2.5 ps (*dashed line*), 12.7 ps (*dotted line*), and 205 ps (*dot-dashed line*).

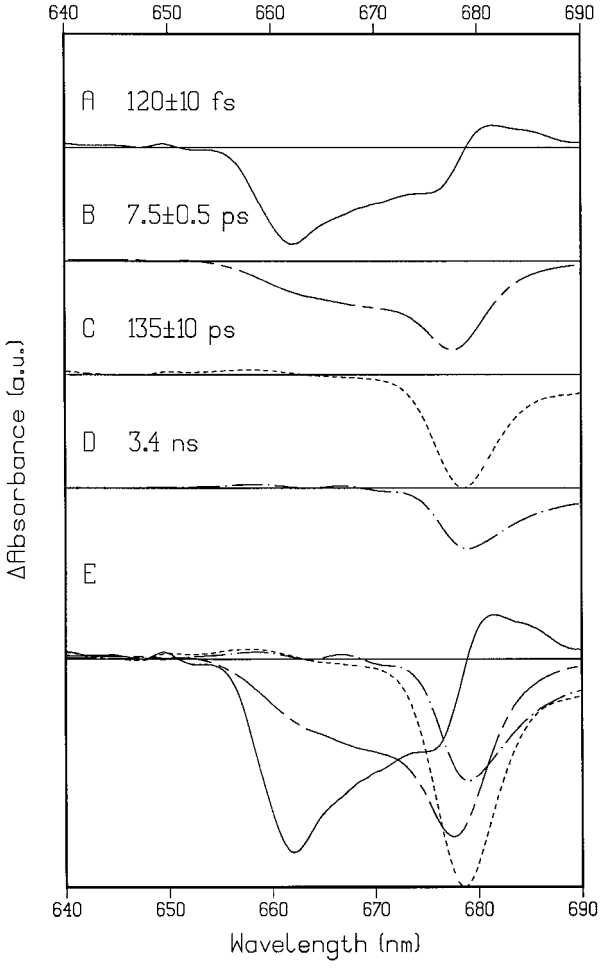

FIGURE 3 Global analysis results of the data presented in short in Fig. 2. A sequential model with four states A $\rightarrow$ B $\rightarrow$ C $\rightarrow$ D was used (see text). The calculated SADS and the lifetimes connecting them are shown in *A–D. E* contains an overlay of all of spectra above.

The spectrum in Fig. 3 *A,* corresponding to the state formed by the excitation pulse, decays into the next one (Fig. 3 *B*) with a time constant of 120 fs, i.e., much faster than the instrument response of the setup. In principle, such a fast process can reflect energy transfer between "blue" and "red" Chl *a* molecules, or relaxation between a higher and a lower excitonic state of a coupled system. There are also other phenomena that may occur on a similar time scale, like relaxation to the lowest vibrational level(s) of the initially excited electronic state(s), coherent coupling between pump and probe pulses, or saturation broadening (Groot et al., 1997). Fitting artifacts and dispersion in the location of time zero across the probing spectrum may contribute as well. Henceforth we will refer to all of these physical or nonphysical fast processes, other than electronic energy transfer, as "ultrafast events." The next SADS (Fig. 3 *B*) still shows a large signal between 660 and 670 nm, in the form of a broad shoulder of the peak situated now at 677.5 nm. With a time constant of 7.5 ps this spectrum evolves into the next one, which has almost no bleaching/SE

due to "blue" Chl *a* left (Fig. 3 *C*). In this spectrum, the maximum is located at 679 nm, and some excited state absorption (ESA) is present around 660 nm. The decay of this quasiequilibrated state is biexponential, with a 135-ps component having a relative amplitude of ~40% and a slower component (fixed to 3.4 ns) accounting for the remaining 60%. Note that some spectral equilibration can be observed during the "fast" phase, but both steps are primarily associated with overall loss of bleaching/SE originating from "red" Chl's.

In the excited-state dynamics studied in this experiment, chlorophylls from several spectral "pools" seem to be involved, either because of direct excitation or because of their role in the energy flow toward a fully equilibrated state. However, in the global analysis of the data described above, it was not possible to unequivocally resolve more than one kinetic component (7.5 ps) associated with EET from "blue" to "red" Chl's *a*. To distinguish more accurately individual transfer processes in LHCII, we prepared a different initial distribution of excited states by using excitation centered at 669 nm. The data presented in Fig. 4 show that the bleaching/SE signal is less broad at early times than in the case of 663-nm excitation, with only two distinct peaks at 670 and 677 nm. In the transient spectra corresponding to delays of 3.3 and 13.3 ps, a gradual decay of the signal around 670 nm is observed together with an ingrowth and a red shift of the bleaching/SE for the other peak. After 38 ps most of the signal is already located around 680 nm, and at later times only an overall decrease of the amplitude is observed.

At least four lifetimes are needed for a satisfactory fit of these data: 0.28 ps, 11.5 ps, 160 ps, and 3.4 ns; the SADS they connect is shown in Fig. 5, *A–E*. The first two time constants are obviously associated with the excitation energy flow from the 670 nm Chl's to the Chl *a*'s absorbing at longer wavelengths, whereas the last two describe the decay of the almost equilibrated state back to the ground state. Yet the subpicosecond step might contain some influence from the "ultrafast events" mentioned above. To estimate this, we

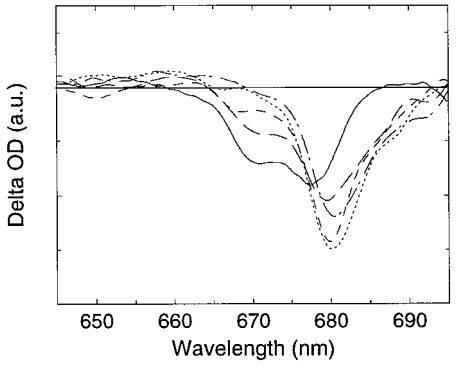

FIGURE 4 Transient absorption difference spectra measured upon 669-nm excitation for the following delays: 0.1 ps (*solid line*), 3.3 ps (*long dashed line*), 13.3 ps (*dashed line*), 38 ps (*dotted line*), and 272 ps (*dot-dashed line*).

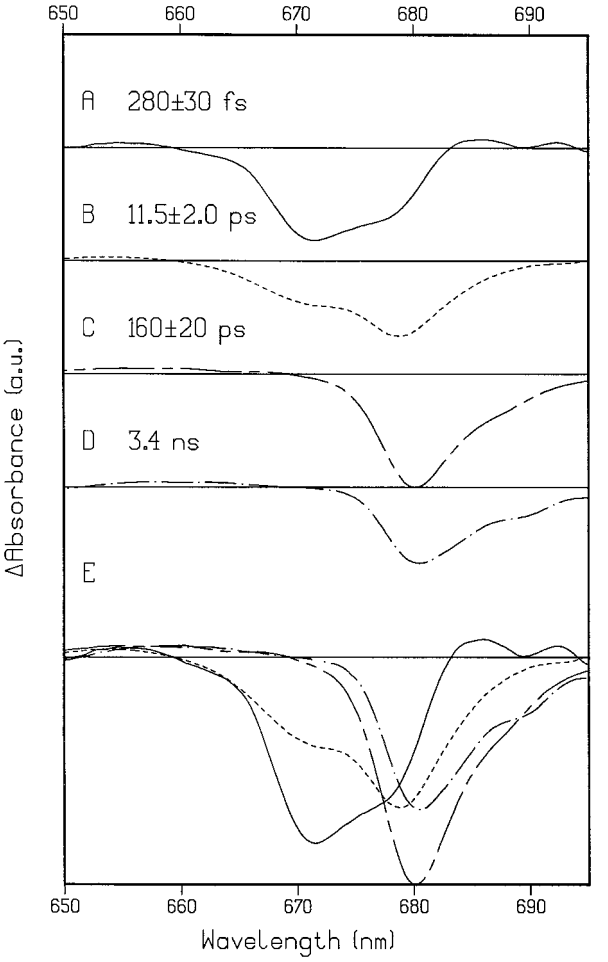

FIGURE 5 SADS and lifetimes resulted from the global analysis of the data, in the case of 669-nm excitation (*A–D*). The number of kinetic components was set to four in the fitting program. *E* shows an overlay of all of the calculated spectra.

modeled the expected bleaching/SE spectrum (not shown) before any EET step occurred, using the approach described in detail for the 663-nm excitation (see Discussion). Because this spectrum and the SADS from Fig. 5 *A* have very similar shapes, it can be concluded that the lifetime of 0.28 ps is largely associated with energy transfer, whereas the other "ultrafast events" show only a minor contribution. Thus this analysis shows that the EET between the 670-nm pigments and the red ones has a biphasic character, with a subpicosecond component whose spectrum peaks around 671 nm, and a relatively slow one (11.5 ± 2.0 ps) that tails down to 660 nm.

The use of excitation pulses centered only 3 nm more to the red, at 672 nm, results in a rather different spectral evolution of the transient absorption spectra. However, the dynamics generally resembles that observed in a similar study on LHCII trimers at 77 K, where 672-nm excitation pulses were used (Visser et al., 1996). When applied to our data, the global analysis routine finds at least four decay times for a satisfactory fit: 65 fs, 0.75 ps, 11 ps, and 215 ps

(Fig. 6). The spectrum from Fig. 6 *A* has a width of ~12 nm (narrower than in case of 669-nm excitation), peaks at 677 nm, and exhibits a shoulder around 673 nm and a small tail between 660 and 665 nm. From this, the next SADS (Fig. 6 *B*) arises during the 0.75-ps process, showing signs of transfer from Chl's absorbing around the pump wavelength to lower energy ones, such as the 2-nm red shift of the maximum, the dropping of the ratio between the shoulder and the maximum, and the ingrowth in the tail of SE (above 685 nm). In the next step (11 ps), connecting spectra 6 *B* and 6 *C,* the maximum shifts further to the red, the shoulders disappear (665 nm) or become very small (673 nm), and the zero-crossing point undergoes a large red shift (~9 nm). Loss of bleaching/SE (probably reflecting singlet-singlet annihilation) is significantly superimposed on both processes above, with an ~70% decrease between the initial and the final state (see, e.g., Fig. 6, *A* and *C*).

Energy equilibration kinetics among the red-most pigments in LHCII monomers was investigated using pump pulses at 678 nm, close to the maximum of the absorption spectrum. Despite the fact that the data primarily show loss of bleaching/SE both on a subpicosecond and a picosecond time scale, a certain amount of equilibration can still be detected. The spectral evolution was fitted with five exponential decays, whose SADS are exhibited in Fig. 7, *A–E.*

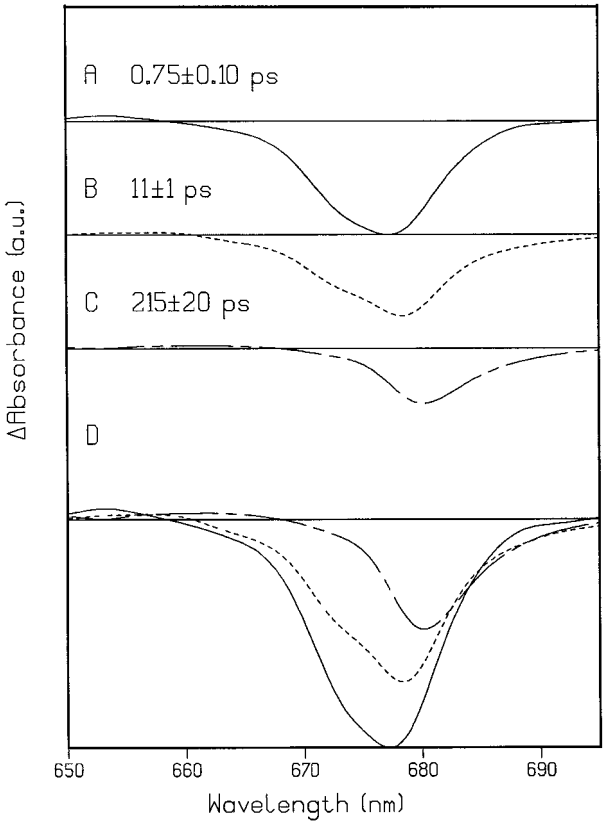

FIGURE 6 Spectral evolution upon 672-nm excitation fitted with four lifetimes: 65 fs, 0.75 ps, 11.1 ps, and 215 ps. The corresponding SADS are shown in *A–C.* The spectrum of the fast decaying artifact (τ = 65 fs) is omitted, and *E* contains an overlay of the spectra shown in *A–C.*

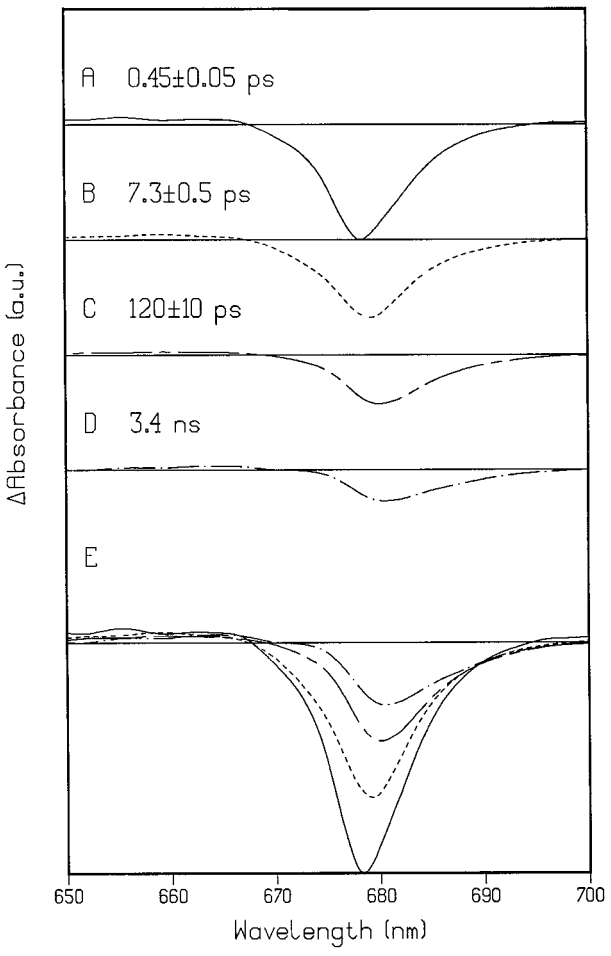

FIGURE 7 Fitting results of the 678-nm excitation data, with five calculated decay times: 70 fs, 0.45 ps, 7.3 ps, 120 ps, and 3.4 ns. The SADS connected by the last four lifetimes are shown separately in *A–D,* and together, for comparison, in *E.*

As in the previous cases, the first spectrum, which decays on a time scale faster than the response time of the setup (less than 100 fs), is not shown. At first glance, the 0.45-ps step is associated with the decay of the bleaching/SE signal in the main absorption band. However, a small red shift of the maximum plus a slight increase in the stimulated emission in the red wing of the next SADS (Fig. 7 *B*) suggests the presence of a fast energy transfer process involving the "blue" and the "red" Chl's of this pool. The spectral equilibration is accomplished over several picoseconds (time constant 7.3 ps), when the blue shoulder of the bleaching disappears and the maximum shifts further to the red (Fig. 7 *C*). A loss process with a time constant of ~120 ps leads to a "final state," which subsequently decays in 3.4 ns back to the ground state. The overall loss of the intensity of bleaching/SE between the initial and the final state was estimated to be ~65%, similar to the case for 672-nm excitation.

In our study of the excited state dynamics in LHCII, the loss processes, such as singlet-singlet annihilation, occur on various time scales and can interfere with energy transfer

processes. To define more accurately the annihilation rates and their influence on EET kinetics, we used excitation in the red wing of the absorption spectrum, at 682 nm. The outcome of the global fit of these data is shown in Fig. 8, *A–D.* Apart from the generally occurring "ultrafast events" (spectrum not shown), the fitting routine finds at least three other decay times. The development of the second SADS from the first takes place with a lifetime of 0.45 ps, a value that is identical to the one found upon 678-nm excitation. The next spectrum (Fig. 8 *C*) appears with a time constant of 60 ps and then disappears on a nanosecond time scale. About 50% of the total bleaching is lost in the first two steps. All of the spectra have a very similar overall shape; only during the 0.45 ps step does some SE appear in the red wing, a sign of a small contribution from energy equilibration. The end spectrum generally resembles the end spectra obtained for all of the previous cases, except that the peak is now shifted 1.5 nm to the red (682 nm).

DISCUSSION

Chl *a*–Chl *a* energy transfer

By selectively exciting various Chl *a* Q_y absorption bands, we have obtained a comprehensive picture of energy equilibration in monomeric LHCII in this spectral region. We will compare it further with the results of similar measurements performed on trimeric LHCII and thus reveal the role of both intra- and intermonomeric interactions in the EET dynamics. Whereas in a previous paper (Kleima et al., 1997) the focus was on Chl *b*–Chl *a* energy transfer, here we address the question how the rates and the amplitudes of the excited-state equilibration involving only Chl *a*'s are affected by the change in aggregation state. Furthermore, as the size of the complex reduces threefold, a better insight into the pigment organization and function in LHCII is obtained, by modeling the observed energy transfer kinetics. Before relating the results of this study to spectroscopic and structural details, such as the absorption spectrum and the orientation of individual pigments, it is essential to discern the lifetimes most likely associated with energy transfer steps.

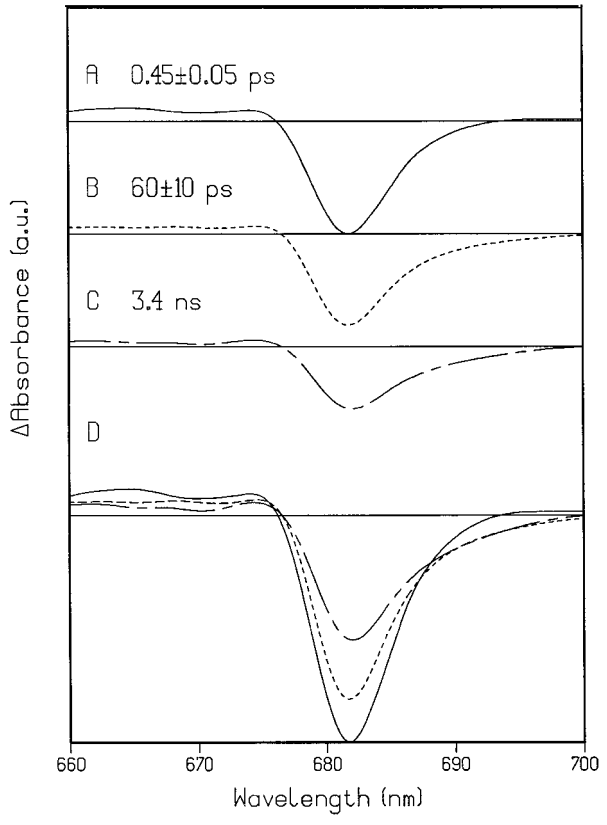

FIGURE 8 Calculated SADS describing the transient absorption changes in the case of excitation at 682 nm (*A–C*), together with the characteristic lifetimes. For clarity, the spectrum of a fast decaying artifact ($\tau \approx 10$ fs) was omitted. *E* shows an overlay of all spectra above.

Upon excitation around 663 nm, two different time constants (120 fs and 7.5 ps) characterize the observed shift of bleaching/SE from 660–670 nm toward the longer wavelengths. The faster time (~120 fs) has not been resolved before in similar experiments on trimers. It may not necessarily be related to energy transfer, because the other "ultrafast events" mentioned above can occur on a similar time scale, which is faster than the instrument response. To identify the nature of the ultrafast component, we approximated the OD spectrum in the 660–700-nm interval by the sum of three spectral "pools," using Chl *a* absorption bands whose phonon wing was derived from fluorescence measurements (Peterman et al., 1997c), with maxima at 677.9, 670.1, and 662.5 nm, respectively (Fig. 9 *A*). The ratios of the areas under these bands are roughly 3:2:1 (677.9 nm: 670.1 nm:662.5 nm), suggesting that the 662.5-nm band is essentially due to only one Chl *a* molecule. Then the pump spectrum (λ_{max} = 663 nm, ~7 nm FWHM) was convoluted with all of these bands to calculate their contribution to the initial excitation, leading to 42% for the 662.5-nm band, 40% for the 670.1-nm band, and 18% for the 677.9-nm band. Using the band deconvolution of the OD spectrum, the contribution of the 662.5-nm band to the initial bleaching/SE spectrum after excitation with a 663-nm pulse (but before any EET step) can be estimated. The SE spectrum is approximated by the mirror image of the absorption band, with a reasonable value of 3 nm for the Stokes' shift. It was assumed that below 665 nm the signal originates only from the 662.5-nm band; for each of the other two bands the bleaching/SE and the ESA cancel each other (compare, e.g., to 669-nm excitation). The estimated contribution of the "blue" band to the SADS from Fig. 3, *A* and *B,* is 65–70% and 30–35%, respectively (see Fig. 9, *B–C*), whereas the expected value, calculated above from the absorption spectrum presuming the absence of excitation transfer towards longer wavelengths, was 42%. Therefore, energy transfer from the blue-most Chl *a* band is essentially described by the 7.5-ps lifetime, whereas the 120-fs component is mainly due to experimental and/or fitting artifacts.

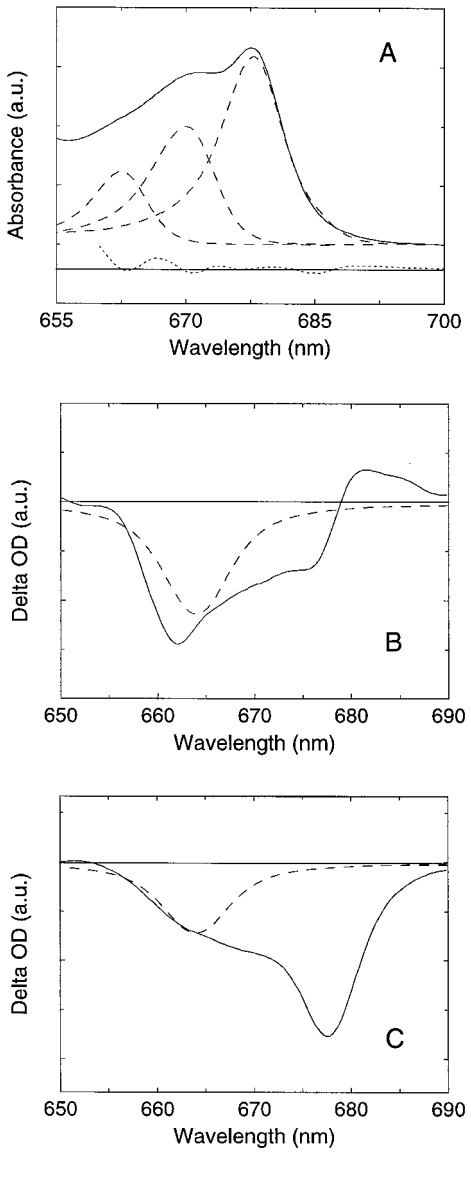

FIGURE 9 (*A*) Approximate description of the OD spectrum of monomeric LHC-II (*solid line*) between 660 and 700 nm, using Chl *a* absorption bands derived by Peterman et al. (1997c). The maxima are at 662.5 nm, 670.1 nm, and 677.9 nm (*dashed lines*), and the residual of the fit is shown below (*dot-dashed line*). (*B*) Comparison between the SADS from Fig. 3 *A* (*solid line*) and the simulated bleaching/SE of the 662.5-nm band only (*dashed line*). (*C*) Comparison between the same simulated spectrum (*dashed line*) and the SADS from Fig. 3 *B* (*solid line*).

Because of the significant amount of direct excitation of the 670-nm Chl's (~40%; see above) and the slow phase of the energy transfer between the 670-nm and 678-nm pools (~12 ps; see Results), the 7.5-ps process is actually a global description of transfer from both 663-nm and 670-nm pigments to the 678-nm ones. Applying the fitting routine only below 665 nm, to minimize the contribution of the 670-nm band, a lower value for the transfer time was found (5 ± 1 ps). This transfer is essentially monoexponential, as expected if the 663-nm absorption band was due mainly to one pigment. In similar experiments performed on trimers, a slightly faster transfer time was observed: 2.4 ps (multicolor pump-probe at 77 K, 662-nm excitation; Visser et al., 1996) or 3 ps (one-color pump-probe for 660 and 665 nm, at 293 K; Kwa et al., 1992). The difference could be caused by factors such as the connection of these "blue" Chl *a*'s to a Chl *a* molecule from another monomeric unit or to the Chl *a* molecule lost during the monomerization procedure. Whatever the nature of the broken connection between the 663-nm pigment and another pigment, the time of transfer to that pigment must be very similar to that of transfer to the remaining pigments (~5 ps), thus explaining the lifetime observed for LHCII trimers (2–3 ps).

Following the approach described above, we obtained the difference absorbance spectrum of the vibrationally relaxed state in the case of 669-nm excitation, assuming that no energy transfer had taken place yet (not shown). Even though the simulated spectrum is somewhat broader than the data (probably because it does not include ESA), its shape globally resembles the shape of the first SADS (Fig. 5 *A*). This suggests that the process occurring with a lifetime of ~0.3 ps must be primarily energy transfer from pigments absorbing around 670 nm to the ones absorbing at longer wavelengths. This value is in agreement with the time constants found for trimeric LHCII: 0.4 ps (Visser et al., 1996) or 0.31 ps (Bittner et al., 1994). Besides this ultrafast component, a considerably slower phase of energy transfer is observed, with a lifetime of ~12 ps. Slow transfer between 670 nm Chl *a*'s and the "red" ones was also detected for LHCII trimers in low-temperature experiments, with characteristic lifetimes of 13 ps (Mullineaux et al., 1993), 14 ps (Bittner et al., 1994), and 15 ± 5 ps (Visser et al., 1995). It was argued that this relatively slow transfer process might involve pigments belonging to different monomeric subunits of the trimer. However, our results support the idea that there are at least two pools of Chl *a*'s showing absorption near 670 nm, whose difference in coupling with neighboring Chl *a* molecules *within* the monomer gives rise to the observed biexponential kinetics (0.3 and 12 ps).

Shifting the pump wavelength slightly to the red to 672 nm results in more direct excitation of the pigments contributing to the main absorption band. Based on the spectral decomposition of the OD spectrum (Fig. 9 *A*), we estimated that ~45% of the initial excitation is localized on the 678-nm band, 50% on the 670-nm band, and only 5% on the 662.5-nm band. As mentioned above, the spectral evolution of the bleaching/SE can be projected onto two exponential components with lifetimes of 0.75 and 11 ps. Both steps occur with significant diminution of the overall signal, probably because of annihilation, but energy transfer features are still present. We believe that the differences in kinetics and in the calculated SADS for this case compared to 669-nm excitation are mostly caused by the interference of the loss processes with the EET events.

If the excitation pulse is centered at 678 nm, fast energy equilibration within the main absorption band takes place with a time constant of ~0.45 ps, also found for 682-nm excitation, which is in agreement with the value found upon

672-nm excitation in trimers (0.42 ps; Visser et al., 1996). Note that in the latter case, a significant amount of main band pigments, absorbing around 676 nm (see Fig. 1, *dashed spectrum*), were directly excited by the pulse centered at 672 nm. In addition, we detected a slower phase of spectral equilibration upon 678-nm excitation, having a characteristic lifetime of ~7.5 ps.

To summarize, in the multicolor pump-probe experiments at 77 K on LHCII monomers, we directly observed downhill energy transfer among Chl *a* states, characterized by at least five lifetimes, spanning two orders of magnitude:

−0.30 ± 0.05 ps, from 670 nm to 680 nm
−0.45 ± 0.05 ps, within the main absorption band
−5 ± 1 ps, from 663 nm to 679 nm (either directly, or via 670 nm)
−7.5 ± 0.5 ps, within the main absorption band
−12 ± 2 ps, from 670 nm to 680 nm

Loss processes in LHCII

One question already raised in previous studies was the extent to which annihilation processes (singlet-singlet or singlet-triplet) affect the excited-state dynamics in LHCII. Annihilation is due to interaction between excited states located on different molecules, in which one molecule relaxes nonradiatively to the ground state while the other one is excited to a higher level. As the latter state returns rapidly to the first excited level, the net result of the process is the loss of one excitation. Experimentally, this manifests itself as an acceleration of the decay of the excited state. In this study, the decay times of the overall bleaching/SE signal for monomeric LHCII that may be associated with singlet-singlet annihilation are 0.45–0.75, 7–11, 60, and 130–160 ps. Note that, like the EET processes described above, the annihilation also takes place over a wide time range. We should mention that the information gathered on the longest lifetime is in general less exact, because the data sets contain 38 delay times, of which only a few extend up to 670 ps. Yet, the end spectra have a similar shape and amplitude for all of the excitation wavelengths (see Results). For photon densities as high as the ones used in this study (0.8–1.5 absorbed photons/monomer) it was shown that in the trimeric LHCII, annihilation may occur for tens or even hundreds of picoseconds (Bittner et al., 1995; Visser et al., 1996). It was suggested that such slow annihilation rates could stem from excitations produced on different monomeric subunits within the trimer. However, these slow processes were now detected on monomeric preparations as well. Understanding these processes in detail requires knowledge about the excited state absorption properties of individual pigments in LHCII, which is lacking, and therefore we will focus below only on the energy transfer processes.

Modeling energy transfer by Förster mechanism

The structural model available for the LHCII complex (Fig. 10) does not provide parameters that are essential for understanding the light-harvesting function, such as the absorption spectrum and the transition dipole orientation of each Chl molecule. The spectral and the kinetic information gathered from probing the energy transfer processes can be used as an effective tool for obtaining more information on these issues. Below we investigate how the observed kinetics can be brought into accordance with available structural information. Because of the binary uncertainty for the dipole orientation of each Chl there are, in principle, 4096 possible configurations for LHCII within the assignment of Chl *a*'s and Chl *b*'s given by Kühlbrandt et al. (1994). At first a filtering procedure is applied, using global knowledge deduced from linear and circular dichroism spectra and from Chl *b*-to-Chl *a* transfer kinetics. Then the solutions are tested to determine whether they can describe the spectral equilibration kinetics in the Chl *a* region observed in our experiments.

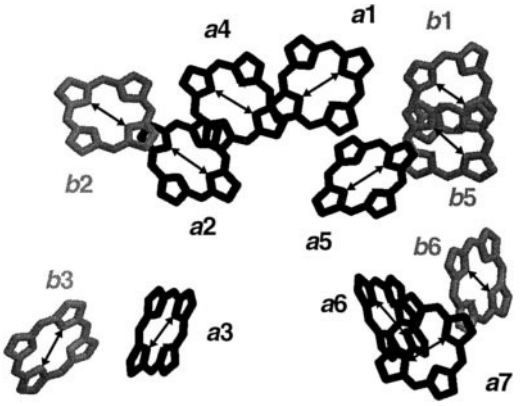

FIGURE 10 Arrangement of chlorophylls in the LHCII monomer, side view. Black, Chl *a*; gray, Chl *b*. The assignment and the notation of each molecule are as given by Kühlbrandt et al. (1994). The arrows indicate the orientation 0 for the Q_y transition dipole moment (see text). The other possible orientation (1) lies along the other diagonal of the porphyrin rings. Note that the orientations found by our filtering procedure are given in Tables 1 and 3.

The coupling strength between Chl *b* and Chl *a* molecules, estimated from the structure, does not exceed 100 cm^{-1} (for a refractive index of 1.3 and optimal orientation), whereas the energy gap between them is more than 400 cm^{-1}. Because of the fact that the Chl *a*'s in the Kühlbrandt model are separated by larger distances, they show a much weaker coupling (less than 30 cm^{-1}). These values are in agreement with the interpigment coupling of ~90 cm^{-1} estimated from CD spectra (Hemelrijk et al., 1992). Thus, concerning the nature of energy transfer in LHCII, the applicability of the Förster mechanism seems justified (see also Visser et al., 1996, and Trinkunas et al., 1997). Coherence effects in the excited state dynamics, such as oscillatory features, have not been observed in LCHII, and if present, they probably do not contribute to processes with lifetimes longer than 0.3 ps. On the other hand, the dipole-dipole approximation used in the Förster formula might not be entirely justified for interpigment distances of 0.8–0.9 nm (in the case of some Chl *b*–Chl *a* pairs), although the

introduced error is probably small (LaLonde et al., 1988). In the following we will consider localized excitations that "hop" between a donor (D) and an acceptor (A) molecule, which are separated by the distance R_{DA} in a medium of refractive index n, with a rate given by the Förster formula (see, e.g., Struve, 1995):

$$k_{DA} = \frac{C_{DA}}{n^4} \cdot (\kappa^2 / R_{DA}^6)$$

The κ^2 factor depends on the orientation of the interacting transition dipole moments as

$$\kappa^2 = [\hat{\mu}_D \cdot \hat{\mu}_A - 3(\hat{\mu}_D \cdot \hat{R}_{DA})(\hat{\mu}_A \cdot \hat{R}_{DA})]^2$$

Here $\hat{\mu}_D$ and $\hat{\mu}_A$ are the unit vectors for the transition dipoles of the donor and the acceptor, respectively, and $\hat{R}_{DA}$ is the unit vector along the direction connecting the "centers" of the two molecules. C_{DA} depends on the overlap integral between the donor's emission (J_D) and the acceptor's absorption (ϵ_A) spectra and is proportional to $\int_0^\infty J_D(\nu)\epsilon_A(\nu)\nu^{-4}d\nu$.

Using the atomic coordinates provided in the structural model (Fig. 10), the distance R between all of the Chl pairs in the LHCII monomer can be calculated. However, the Q_y transition dipole moment, which appears in the κ^2 expression, can assume two possible orientations for each molecule: 0 or 1, i.e., along the NA-NC axis or the NB-ND axis, respectively (nomenclature as in Gülen et al., 1997). The C_{DA} coefficients for Chl *a*–Chl *a* (C_{aa}), Chl *b*–Chl *b* (C_{bb}), Chl *b*–Chl *a* (C_{ba}), and Chl *a*–Chl *b* (C_{ab}) pairwise transfers are estimated using the method suggested originally by Shipmann and Hausmann (1979) and later modified by Jean et al. (1988). This is an analytical method that approximates the absorption and emission spectra as symmetric Gaussians, operating with parameters like spectral width (σ), peak wavelength (λ), and transition dipole strength (μ). Thus it has been shown (Jean et al., 1988) that for a Chl pair whose emission and absorption maxima are separated by Δ_{DA},

$$C_{DA} = \mu_D^2 \cdot \mu_A^2 \cdot I_{DA}$$

with

$$I_{DA} = \text{constant} \cdot \frac{1}{\sqrt{2\pi(\sigma_D^2 + \sigma_A^2)}} \cdot \exp[-\Delta_{DA}^2/2(\sigma_D^2 + \sigma_A^2)]$$

where the constant is 29.99 Debye^{-4} ps^{-1} nm^6 cm^{-1}.

Because no reliable values for most of these parameters in LHCII are available, we used the ones from the absorption/emission data of Chl's in solution (CCl_4) at room temperature (Sauer et al., 1966): the spectral widths σ_a = 135 cm^{-1} and σ_b = 145 cm^{-1}, the dipole strengths μ_a^2 = 24.65 Debye^2 and μ_b^2 = 16.91 Debye^2, and the separations $\Delta_{aa} = \Delta_{bb}$ = 110 cm^{-1}, Δ_{ba} = 275 cm^{-1} and Δ_{ab} = 495 cm^{-1}. With these parameters, we estimated that C_{aa} = 32.26, C_{bb} = 14.45, C_{ba} = 9.61, and C_{ab} = 1.11 nm^{6}ps^{-1}, values that are in agreement with earlier calculations based on experimental spectra, for LHCII trimers at 77 K (Visser et al., 1996). After checking thoroughly that the obtained conclusions do not depend on the precise choice of the spectral parameters, we assumed for simplicity that all of the Chl *b* (*a*) are spectrally equivalent, with the Q_y transitions around 650 nm for Chl *b* and 670 nm for Chl *a* (but see below). The use of room temperature spectra is justified by the fact that the measured energy transfer rates from Chl *b* to Chl *a* in LHCII were found to be almost independent of temperature (see, e.g., Visser et al., 1996, and Connelly et al., 1997b) and by the fact that the calculated downhill rates are rather insensitive to temperature between 0 and 300 K (Struve et al., 1995).

Using the correct value for the refractive index in the Förster formula is a nontrivial issue, as discussed, for instance, by Moog et al. (1984). In our case it is used merely as a scaling factor, i.e., a value of 1.55 leads to a range of calculated transfer times that is in agreement with the one obtained experimentally (0.2–20 ps). The calculated rates were further used in the Pauli master equation (see, e.g., Struve, 1995), which gave the time-dependent occupation probabilities $P_i(t)$ for each molecule i (i = 1–12). Then the quantity whose dynamics is used below to describe the Chl *b*-to-Chl *a* energy transfer is defined as $P_b(t) = \Sigma_{bi}P_{bi}(t)$ (the summation is taken over all Chl *b* molecules).

An additional criterion for resolving the ambiguities in the dipole moment orientations takes advantage of the sensitivity of polarized absorption spectroscopy (linear and circular dichroism) to the molecular configuration. A set of restrictions can be imposed on the overall shape of the circular dichroism and on the magnitude of the reduced linear dichroism produced by the Chl *a* and Chl *b* molecules in the Q_y region, based on experimental spectra (Hemelrijk et al., 1992; van Amerongen et al., 1994). Thus it was proved that by using relatively mild restrictions, the number of allowed configurations in the Kühlbrandt model can already be reduced considerably, from 4096 to less than 100, meaning that ~4000 combinations of dipole orientations can definitely not explain the observed linear dichroism (LD) and circular dichroism (CD) spectra of LHCII (Gülen et al., 1997).

Our extended approach consists of a complete search in the space of possible orientations using a set of very general filtering criteria, derived not only from the steady-state polarized absorption spectra, but also from the Chl *b*-to-Chl *a* transfer dynamics:

1. The values of the reduced linear dichroism are $LD_a < -0.1$ and $|LD_b| < |LD_a|$, where LD_b is the average over 640 nm $< \lambda <$ 660 nm, and LD_a is the average for $\lambda >$ 660 nm (see also van Amerongen et al., 1994, and Gülen et al., 1997).

2. The CD spectrum has a biphasic character in the Chl *a* region, with a positive sign on the short wavelength side (see also Gülen et al., 1997).

3. Approximately 20% of the Chl *b*-to-Chl *a* energy transfer is "slow" (several picoseconds), whereas the remaining 80% should not be entirely "fast" (less than 0.4 ps)

TABLE 1 Selected LHCII configurations within the Kühlbrandt model

No.	*a*1	*a*2	*a*3	*a*4	*a*5	*a*6	*a*7	*b*1	*b*2	*b*3	*b*5	*b*6	LD_a	LD_b	$b \rightarrow a$
2994	0	1	0	0	0	1	0	0	1	1	1	0	−0.117	−0.016	−
3002	0	1	0	0	0	1	0	0	0	1	1	1	−0.136	0.022	−
3057	0	1	0	0	0	0	0	0	1	1	1	1	−0.131	0.103	+
3058	0	1	0	0	0	0	0	0	1	1	1	0	−0.155	−0.026	+
3065	0	1	0	0	0	0	0	0	0	1	1	1	−0.149	0.142	−
3066	0	1	0	0	0	0	0	0	0	1	1	0	−0.172	0.013	+
4018	0	0	0	0	0	1	0	0	1	1	1	0	−0.165	0.098	−
4026	0	0	0	0	0	1	0	0	0	1	1	0	−0.130	−0.016	−
4082	0	0	0	0	0	0	0	0	1	1	1	0	−0.198	0.089	−

Notation and selection criteria are as given in the text; Chl assignment is as in Fig. 10. The sign + means that the transfer time for two Chl *b*'s is "fast" (0.2–0.4 ps) and that for the other two is "intermediate" (0.5–0.8 ps). The configurations with − obey only milder restrictions on the transfer kinetics, i.e., 60% of it is either "fast" or "intermediate." In all cases, a "slow" component (2–5 ps), with a relative amplitude of 20%, originates from the *b*5 pigment. As required by the filtering criteria, the transfer time from *b*3 to *a*3 is "fast" (0.27 ps). The decay of the excited state on *b*1 is always "intermediate" (transfer time $\tau = 0.65$ ps, toward *a*1). With only one exception (when both *b*2 and *a*2 are in orientation 1, $\tau = 0.57$ ps), *b*2 shows a "fast" transfer toward *a*2 ($\tau = 0.22$–0.27 ps), whereas *b*6 has a "fast" EET rate to the *a*6–*a*7 pair in orientation 1 and an "intermediate" one otherwise.

or completely "intermediate" (0.5–0.8 ps) (see, e.g., Visser et al., 1996, and Connelly et al., 1997b).

4. The transfer time between *b*3 and *a*3 is "fast" (0.3–0.45 ps), and *b*3 is in configuration 1, as concluded from LD and femtosecond measurements on a closely related protein, CP29 (Gradinaru et al., 1998).

The configurations that comply with these requirements are subsequently tested for the energy equilibration kinetics between Chl *a* pigments, using the information provided by this study and assuming a certain spread in the energy of their Q_y transition (663 nm $< \lambda_{max} <$ 678 nm). This spread leads to only small changes in the calculated Förster rates for Chl *b*-to-Chl *a* transfer, but it gives a certain directionality to the energy transfer between various Chl *a* pools at 77 K.

The result of the filtering procedure based on the criteria listed above, taking into account the Chl assignment proposed by Kühlbrandt et al. (see Fig. 10), is presented in Table 1. Of the total of nine surviving configurations, only three are rigorous solutions (graded with + in the table), whereas the other six obey only somewhat milder restrictions. One can see that a large number of pigments prefer only one of the two possible orientations for their Q_y transition dipole, i.e., *a*1, *a*3, *a*4, *a*5, *a*7, and *b*1 assume the orientation 0, whereas *b*3 and *b*5 are found in orientation 1. The remaining molecules (*a*2, *a*6, *b*2, and *b*6) can be found in both 0 and 1 orientations. This is clearly illustrated in Table 2, which shows the reduction strength of each of the imposed criteria, together with the tendency of each Chl to assume one of the two available orientations, 0 or 1.

We will further discuss the possible energy transfer pathways and the role of each Chl molecule in terms of the compartmental nature of the selected configurations, which was brought to our attention by Dr. R. Knox (personal communication). Here, "compartment" refers to a group of pigments "equilibrating" very fast ($\tau \lesssim 1$ ps) and significantly slower ($\tau \gtrsim 5$ ps) with the rest of the pigments in the complex. Based on this definition, we identified the following four compartments within the LHCII monomer that are common to all configurations given in Table 1:

compartment 1: *b*1, *b*2, *a*1, and *a*2
compartment 2: *b*3 and *a*3
compartment 3: *a*4 and *a*5
compartment 4: *b*6, *a*6, and *a*7

The Chl *b*5 is connected to *a*5 ($\tau \simeq 5$ ps) and, in some cases, to compartment 4 ($\tau = 2$–3 ps, if *b*6 is in the 0 orientation). Note that within the compartments there might be some delocalization of excitations, but equilibration remains ultrafast.

For all cases above, *a*3 is the only "unpaired" Chl *a*, with a calculated transfer time to the rest of the monomer of ~5

TABLE 2 Survival statistics—Kühlbrandt model

Filtering criteria	Survivors	*a*1	*a*2	*a*3	*a*4	*a*5	*a*6	*a*7	*b*1	*b*2	*b*3	*b*5	*b*6
LD_a	397	0.806	0.620	0.408	0.907	0.730	0.763	0.980	0.499	0.448	0.519	0.509	0.683
LD_{ab}	102	0.961	0.539	0.461	0.951	0.716	0.706	1.00	0.716	0.529	0.010	0.402	0.882
$LD_{ab} + CD_a$	46	1.00	0.217	0.565	0.978	0.957	0.587	1.00	0.652	0.478	0.022	0.435	0.891
$LD_{ab} + CD_a + CP$	25	1.00	0.360	1.00	1.00	0.920	0.560	1.00	0.680	0.480	0.000	0.360	0.920
$LD_{ab} + CD_a + CP + EET$	9	1.00	0.333	1.00	1.00	1.00	0.556	1.00	1.00	0.444	0.000	0.000	0.778

Probabilities of being in orientation 0 are listed for each Chl molecule, normalized with respect to the total number of survivors in each row. In the first column, LD_a is the restriction imposed on the reduced linear dichroism of the Chl *a*'s. LD_{ab} further includes the criteria for the Chl *b*'s. CD_a refers to the circular dichroism requirements, and EET is related to the excitation transfer pattern from Chl *b* to Chl *a* pigments (see text). CP denotes a restriction derived from ultrafast spectroscopy on CP29 (Gradinaru et al., 1998), i.e., *b*3 is in orientation 1 and *a*3 is in orientation 0. The last nine survivors are the ones shown in Table 1.

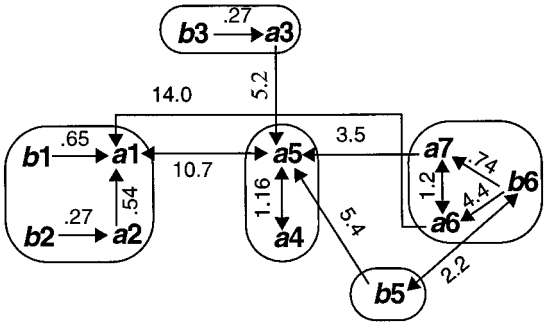

FIGURE 11 Block-diagram representation of the energy transfer kinetics in LHCII, for the following Chl spectra and orientations (configuration 3066, Table 1): $a1 \approx 678$ nm (0), $a2 \approx 671$ nm (1), $a3 \approx 662$ nm (0), $a4/a5 \approx 678$ nm (0), $a6 \approx 670$ nm (0), $a7 \approx 667$ nm (0), $b1/b2 \approx 650$ nm (0), $b3 \approx 640$ nm (1), $b5 \approx 650$ nm (1), and $b6 \approx 650$ nm (0).

ps. Because the 663-nm absorption band has a dipole strength corresponding to approximately one pigment (see above), the transfer kinetics observed upon 663-nm excitation ($\tau \simeq 5$ ps) can be explained only if *a*3 is assigned to this "blue" Chl *a*. Any other assignment would unavoidably lead to fast equilibration within a compartment having two Chl *a*'s (including species absorbing at longer wavelengths), thus contradicting the experimental results. Furthermore, the slow EET phase from the 670-nm to the 678-nm pool ($\tau \simeq 12$ ps) can only be ascribed to transfer between different compartments, implying that both Chl *a*'s in one of the compartments 1, 3, or 4 should belong to the 670-nm pool. Then, one more Chl *a* molecule in the remaining compartments should also absorb near 670 nm, to explain the presence of the subpicosecond lifetime observed upon 669-nm excitation (see, e.g., Fig. 5). One of the solutions (dipole orientations and spectral assignment) that gives a satisfactory description of the observed energy transfer kinetics in the Chl *a* region is presented in Fig. 11.

However, there is an important shortcoming for this solution that actually holds for all configurations selected within the Kühlbrandt model of LHCII. Based on transient absorption measurements on CP29 (Gradinaru et al., 1998), it was concluded that *a*3 must be a "red" pigment (675–680 nm), whereas, to explain the energy transfer kinetics for LHCII, we should now put its maximum near 663 nm. A large shift of the absorption of this molecule in LHCII versus CP29 is unlikely to occur, given the high degree of sequence homology between the two antennae.

From a reconstitution study on CP29, in which site-directed mutations prevented certain Chl molecules from binding, it was concluded that the Chl *b* molecule corresponding to Chl *b*5 from LHCII is in fact a Chl *a* (Dr. R. Bassi, personal communication). Furthermore, based on the results of that study and on the assumption that similar binding sites in LHCII and CP29 bind identical pigments, it should be concluded that in LHCII only one of the Chl's *b*1, *b*2, *a*6, and *a*7 must be a Chl *a*, to conserve the numbers of Chl *a* and *b* per monomer (seven and five, respectively). For *b*1, *b*2, or *a*6 being a Chl *a*, an unreasonably high proportion of the Chl *b*-to-Chl *a* transfer (40–60%) would take place on a picosecond time scale, if simultaneously the dichroic criteria have to be fulfilled. Only in the case in which the molecules *b*5 and *a*6 of the Kühlbrandt model have swapped their identities (next they will be named $a6_{b5}$ and $b5_{a6}$, respectively) can 15 configurations be found that obey all restrictions listed above (see Table 3). The reduction statistics for this model are shown in Table 4.

The only configuration with *a*5 in the orientation 1 (2860) can be ruled out, because the calculated transfer times between Chl *a*'s are much longer than the experimental values. Therefore, we will further discuss only the remaining 14 configurations, which are organized in four classes with respect to the Chl *a* orientations: 26, 2, 6, and ∅ (the names refer to the Chl *a*'s found in orientation 1, i.e., *a*2

TABLE 3 Selected LHCII configurations within a modified Kühlbrandt model

No.	*a*1	*a*2	*a*3	*a*4	*a*5	*a*6	*a*7	*b*1	*b*2	*b*3	*b*5	*b*6	LD_a	LD_b	$b \rightarrow a$
2860	*0*	*1*	*0*	*0*	*1*	*1*	*0*	*1*	*0*	*1*	*0*	*0*	*−0.105*	*0.076*	+
2978	0	1	0	0	0	1	0	1	1	1	1	0	−0.124	−0.092	−
2980	0	1	0	0	0	1	0	1	1	1	0	0	−0.114	−0.002	−
2988	0	1	0	0	0	1	0	1	0	1	0	0	−0.139	0.043	+
2994	0	1	0	0	0	1	0	0	1	1	1	0	−0.128	−0.003	−
2996	0	1	0	0	0	1	0	0	1	1	0	0	−0.120	−0.100	−
3004	0	1	0	0	0	1	0	0	0	1	0	0	−0.142	−0.057	+
3058	0	1	0	0	0	0	0	0	1	1	1	0	−0.131	0.034	−
3060	0	1	0	0	0	0	0	0	1	1	0	0	−0.123	−0.054	−
3068	0	1	0	0	0	0	0	0	0	1	0	0	−0.141	−0.023	+
4004	0	0	0	0	0	1	0	1	1	1	0	0	−0.163	0.114	+
4012	0	0	0	0	0	1	0	1	0	1	0	0	−0.128	0.002	+
4020	0	0	0	0	0	1	0	0	1	1	0	0	−0.165	0.004	+
4082	0	0	0	0	0	0	0	0	1	1	1	0	−0.176	0.139	−
4084	0	0	0	0	0	0	0	0	1	1	0	0	−0.169	0.046	+

The pigments *a*6 and *b*5 in the Kühlbrandt model (Fig. 10) have their identities swapped. The signs + and − in the last column have the same meaning as in Table 1. The Chl's *b*2 and *b*3 show the same decay pattern as discussed for Table 1. In all cases, *b*6 has an "intermediate" transfer time toward *a*7 (0.74 ps), which also receives excitation from *b*5 (either directly or via *b*6). Chl *b*1 shows an "intermediate" transfer time to either *a*1 or *a*6, depending on its dipole orientation. The configuration shown in italics is ruled out on the basis of Chl *a*–Chl *a* energy transfer (see text).

TABLE 4 Survival statistics—a modified Kühlbrandt model

Filtering criteria	Survivors	*a*1	*a*2	*a*3	*a*4	*a*5	*a*6	*a*7	*b*1	*b*2	*b*3	*b*5	*b*6
LD_a	285	0.835	0.656	0.379	0.993	0.761	0.414	1.00	0.446	0.439	0.530	0.488	0.702
LD_{ab}	77	1.00	0.532	0.519	1.00	0.870	0.455	1.00	0.649	0.519	0.065	0.584	0.883
LD_{ab} + CD_a	51	1.00	0.314	0.588	1.00	0.980	0.333	1.00	0.647	0.529	0.078	0.588	0.863
LD_{ab} + CD_a + CP	27	1.00	0.370	1.00	1.00	0.963	0.370	1.00	0.593	0.519	0.000	0.593	0.889
LD_{ab} + CD_a + CP + EET	15	1.00	0.313	1.00	1.00	0.938	0.375	1.00	0.563	0.313	0.000	0.688	1.00

The filtering criteria are the same as in Table 2, and the modifications in the pigment assignment are as described in the text. The probability of being in the 0 orientation is given for each chlorophyll, normalized with respect to the total number of survivors in each row. The last 15 configurations are the ones given in Table 3.

and/or $a6_{b5}$). Note that seven pigments have, in all cases, a conserved orientation: *a*1, *a*3, *a*4, *a*5, *a*7, and *b*6 are in 0, where *b*3 is in 1 (see, e.g., Tables 3 and 4). Furthermore, the only four configurations with $b5_{a6}$ in orientation 1 have the worst "grades" for Chl *b*-to Chl *a* transfer, so it is quite likely that the Q_y transition dipole of Chl $b5_{a6}$ lies along the 0 direction. The solutions share a common compartmental structure, which is to a large extent similar to the one discussed above:

compartment 1: *a*1, *a*2, and *b*2
compartment 2: *a*3 and *b*3
compartment 3: *a*4, *a*5, and $a6_{b5}$
compartment 4: *a*7, $b5_{a6}$, and *b*6

For orientation 0 Chl *b*1 belongs to compartment 1, whereas for orientation 1 it is found in compartment 3, connected to $a6_{b5}$.

For two Chl *a* configurations (6 and 26), *a*7 shows a transfer time of 3–4 ps toward *a*5, a value that approaches the transfer time observed upon 663-nm excitation (~5 ps). A possible solution, in which both the fast and the slow energy transfer rates and their associated spectral features are consistent with the experimental observations, can be obtained by assigning *a*7 to the 663-nm absorption band, as shown in Fig. 12. Compared to the Kühlbrandt model, in this case the *a*3 pigment can have an absorption peak that is close to the one inferred from fast measurements on CP29.

However, for the other two Chl *a* configurations (2 and ∅), it is necessary to place *a*3's absorption around 663 nm to explain the observed transfer time from this wavelength to the red, leading again to the already discussed disagreement concerning the spectral assignment of *a*3 in LHCII versus CP 29. As a global feature, for all configurations listed in Table 3, the calculated LD_a and LD_b values are closer to the experimental ones than for the other case (see, e.g., Table 1).

Finally, we want to comment on the role of each compartment in the in vivo energy transfer pathways in LHCII, for the two Chl assignments discussed above. LHCII in vivo is probably an aggregated form of the trimeric LHCII. One therefore expects three levels of energy transfer: transfer within a monomer, transfer within a trimer, and transfer between trimers. As shown in a recent study (Kleima et al., 1997), the Chl *b*-to-Chl *a* transfer is essentially taking place within the monomeric subunit of the trimer, mostly on a subpicosecond time scale. This corresponds to the fast transfer rates between Chl's *b* and *a* within the same compartments. Furthermore, the Chl *a* spectral equilibration in monomers is very similar to that observed in trimers, with lifetimes ranging from 300 fs to 12 ps. The faster rates probably originate from intracompartmental Chl *a* pairs, whereas the slower ones are due to transfer between compartments. Upon examining the block diagrams of all configurations selected above (figures not shown), it becomes apparent that compartment 3 (*a*4–*a*5, plus $a6_{b5}$ for the modified model) can exchange excitation energy with all of the other compartments within the same monomer. This is mainly due to good connections of *a*5 to *a*1 (τ = 10.67 ps), *a*3 (τ = 5.22 ps), and *a*7 (τ = 3.49 ps), but also, in some configurations, to the *a*4–*a*2 coupling (τ = 5.39 ps) or to the $a6_{b5}$–*a*7 coupling (τ = 2.65 ps). Moreover, the strongest intermonomeric connection is between Chl's *a*4 and *a*5 from adjacent monomeric subunits of the trimer (τ = 16.23 ps, when both pigments are in the 0 orientation), thus suggesting that compartment 3 is important for intermonomeric energy transfer. Meanwhile, the Chl *a* molecules in compartments 1 and 4 are close to the periphery of the trimeric complex, so at least some of them could be the main exit points to other trimers.

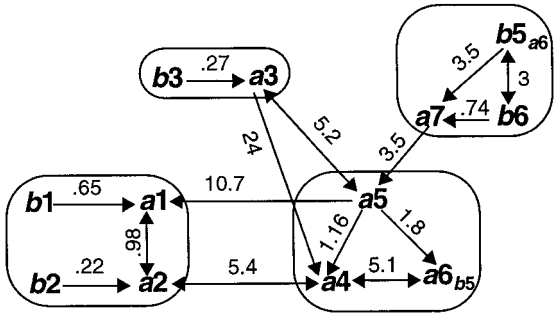

FIGURE 12 Block-diagram representation of energy transfer in LHCII in a modified version of the Kühlbrandt model, for the following spectral and orientational assignment (configuration 4020, Table 3): *a*1/*a*2 ≈ 678 nm (0), *a*3 ≈ 672 nm (0), *a*4 ≈ 678 nm (0), *a*5 ≈ 667 nm (0), $a6_{b5}$ ≈ 678 nm (1), *a*7 ≈ 662 nm (0), *b*1 ≈ 650 nm (0), *b*2 ≈ 650 nm (1), *b*3 ≈ 640 nm (1), $b5_{a6}$/*b*6 ≈ 650 nm (0). Note that the names of molecules *a*6 and *b*5 are interchanged as compared to Fig. 10.

CONCLUSIONS

In this transient absorption study several energy transfer processes occurring among the Chl *a* molecules of the monomeric subunit of the LHCII were identified. The rates and their associated spectra show remarkable similarity to the results of previous measurements performed on trimers, demonstrating that the spectral equilibration kinetics is almost entirely determined by intramonomeric energy transfer. On the other hand, it is inferred that the lifetimes associated with intermonomeric transfer are no less than 10 ps. To understand the role of each Chl *a* in the process of light harvesting and to identify possible pathways for the energy flow in the LHCII complex, we modeled the energy transfer using the Förster mechanism. Then a complete search in the large space of possible combinations of individual dipole orientations was performed, using a set of relatively mild criteria derived from both dichroic and pump-probe measurements on LHCII and CP29.

Assuming the validity of Kühlbrandt's assignment of the Chl's in LHCII, just a limited number of configurations (nine) was not immediately rejected, with only four pigments lacking a uniquely determined orientation for their Q_y transition dipole (*a*2, *a*6, *b*2, and *b*6). The dipole orientations for the other Chl's were as follows: 0 for *a*1, *a*3, *a*4, *a*5, *a*7, and *b*1, and 1 for *b*3 and *b*5. Hence, in terms of Chl *a* orientations, the surviving configurations were all reduced to just four different combinations. In all of them Chl *a*3 should absorb near 663 nm to be consistent with the observed EET kinetics, an assignment that is incompatible with the CP29 result (*a*3 at 675–680 nm).

The same searching procedure was applied to modified Kühlbrandt models, assuming that, as in CP29, *b*5 is a Chl *a* ("$a6_{b5}$"). Only the model in which *a*6 is a Chl *b* ("$b5_{a6}$") was found to be consistent with the steady-state and kinetic observations. In this case 14 configurations survived, with the dipole orientations determined for most of the pigments: 1 for *b*3, and 0 for *a*1, *a*3, *a*4, *a*5, *a*7, and *b*6 (and probably $b5_{a6}$ as well; see Discussion). For only nine of these combinations (when $a6_{b5}$ is in 1) was it possible to avoid the inconsistency regarding the spectral assignment of *a*3, by choosing *a*7 to be the Chl *a* absorbing near 663 nm. The kinetic and spectral features of the observed EET were satisfactorily reproduced in this case, and a relatively better description of the dichroic spectra was obtained (see Table 3). However, our filtering procedure does not yield an unambiguous solution for the pigment assignments and orientations, but provides a very restricted set of possible configurations. This is caused by several factors, such as the complexity of the system, the limited spectroscopic information, and the mildness of the selection criteria. As can be seen in Tables 2 and 4, almost all Q_y transitions can be determined with confidence if a certain assignment for the chlorophyll identities is adopted.

For the solutions discussed above, the compartmental pattern of energy transfer in LHCII becomes evident, with energy equilibration taking place first locally (with only a few pigments involved), on a subpicosecond time scale, and then globally (with the rest of the complex), over many picoseconds. Dichroic and pump-probe measurements on well-defined mutants will probably prove essential for a full understanding of energy transfer routes in LHCII. Using the results of this study, we are in a position to make predictions on what to expect if the energy transfer paths are reengineered, for instance, if certain Chl's are prevented from binding. In the future, combining this with a more refined numerical procedure to include spectral details and some (limited) excitonic effects will, without doubt, help in resolving the issues left unsettled by the current approach.

The authors thank F. Calkoen for isolating the LHCII monomers and Dr. Roberto Bassi (Università di Verona, Verona, Italy) for providing valuable information about the pigment assignment in CP29. We also acknowledge Dr. Robert Knox (University of Rochester) for inspiring discussions on the compartmental nature of the selected configurations. CCG was supported by grant 1932802 from the Human Frontier Science Program Organisation. DG is grateful to the Nederlandse Organisatie voor Wetenschappelijk Onderzoek (NWO) for providing financial support.

REFERENCES

Bittner, T., G. P. Wiederrecht, K.-D. Irrgang, G. Renger, and M. Wasielewski. 1994. Ultrafast excitation energy transfer and exciton-exciton annihilation processes in isolated light harvesting complexes of photosystem II (LHC II) from spinach. *J. Phys. Chem.* 98:11821–11826.

Bittner, T., G. P. Wiederrecht, K.-D. Irrgang, G. Renger, and M. Wasielewski. 1995. Femtosecond transient absorption spectroscopy on the light-harvesting Chl *a*/*b* protein complex of photosystem II at room temperature and 12 K. *Chem. Phys.* 194:312–322.

Connelly, J. P., M. G. Müller, R. Bassi, R. Croce, and A. R. Holzwarth. 1997a. Femtosecond transient absorption study of carotenoid to chlorophyll energy transfer in the light-harvesting complex II of photosystem II. *Biochemistry.* 36:281–287.

Connelly, J. P., M. G. Müller, M. Hucke, G. Gatzen, C. W. Mullineaux, A. V. Ruban, P. Horton, and A. R. Holzwarth. 1997b. Ultrafast spectroscopy of trimeric light-harvesting complex II from higher plants. *J. Phys. Chem. B.* 101:1902–1909.

Gradinaru, C. C., A. A. Pascal, F. van Mourik, B. Robert, P. Horton, R. van Grondelle, and H. van Amerongen. 1998. Ultrafast evolution of the excited states in the chlorophyll a/b complex CP29 from green plants studied by energy-selective pump-probe spectroscopy. *Biochemistry.* 37:1143–1149.

Groot, M. L., R. van Grondelle, J. A. Leegwater, and F. van Mourik. 1997. Radical pair quantum yield in reaction centers of photosystem II of green plants and the bacterium *Rhodobacter sphaeroides*—saturation behaviour with sub-picosecond pulses. *J. Phys. Chem. B.* 101:7869–7873.

Gülen, D., R. van Grondelle, and H. van Amerongen. 1997. Structural information on the light-harvesting complex II of green plants that can be deciphered from polarized absorption characteristics. *J. Phys. Chem. B.* 101:7256–7261.

Hemelrijk, P. W., S. L. S. Kwa, R. van Grondelle, and J. P. Dekker. 1992. Spectroscopic properties of LHCII, the main light-harvesting chlorophyll *a*/*b* protein complex from chloroplast membranes. *Biochim. Biophys. Acta.* 1098:159–166.

Jean, J. M., C. K. Chan, and G. R. Fleming. 1988. Electronic energy transfer in photosynthetic bacterial reaction centers. *Isr. J. Chem.* 28: 169–175.

Kleima, F. J., C. C. Gradinaru, F. Calkoen, I. H. M. van Stokkum, R. van Grondelle, and H. van Amerongen. 1997. Energy transfer in LHC-II monomers at 77K studied by sub-picosecond transient absorption spectroscopy. *Biochemistry.* 36:5262–5268.

Krawczyk, S., Z. Krupa, and W. Maksymiec. 1993. Stark spectra of chlorophylls and carotenoids in antenna pigment-proteins LHC-II and CP-II. *Biochim. Biophys. Acta.* 1143:273–281.

Kühlbrandt, W., D. N. Wang, and Y. Fujiyoshi. 1994. Atomic model of plant light-harvesting complex by electron crystallography. *Nature.* 367: 614–621.

Kwa, S. L. S., H. van Amerongen, S. Lin, J. P. Dekker, R. van Grondelle, and W. S. Struve. 1992. Ultrafast energy transfer in LHC-II trimers from the Chl *a*/*b* light-harvesting antenna of photosystem II. *Biochim. Biophys. Acta.* 1101:202–212.

LaLonde, D. E., J. D. Petke, and G. M. Maggiora. 1988. Evaluation of approximation in molecular exciton theory. 1. Applications to dimeric systems of interest in photosynthesis. *J. Phys. Chem.* 92:4746–4752.

Moog, R. S., A. Kuki, M. D. Fayer, and S. Boxer. 1984. Energy transport and trapping in a synthetic chlorophyllide substituted hemoglobin: the orientation of the chlorophyll S1 dipole. *Biochemistry.* 23:1564–1571.

Mullineaux, C. W., A. A. Pascal, P. Horton, and A. R. Holzwarth. 1993. Excitation-energy quenching in aggregates of the LHC II chlorophyll-protein complex: a time-resolved fluorescence study. *Biochim. Biophys. Acta.* 1141:23–28.

Nussberger, S., J. P. Dekker, W. Kühlbrandt, B. M. Bolhuis, R. van Grondelle, and H. van Amerongen. 1994. Spectroscopic characterization of three different monomeric forms of the main chlorophyll *a*/*b* binding protein from chloroplast membranes. *Biochemistry.* 33:14775–14783.

Peterman, E. J. G., F. M. Dukker, R. van Grondelle, and H. van Amerongen. 1995. Chlorophyll *a* and carotenoid triplet states in light harvesting complex II of higher plants. *Biophys. J.* 69:2670–2678.

Peterman, E. J. G., C. C. Gradinaru, F. Calkoen, J. C. Borst, R. van Grondelle, and H. van Amerongen. 1997a. Xantophylls in light-harvesting complex II of higher plants: light harvesting and triplet quenching. *Biochemistry.* 36:12208–12215.

Peterman, E. J. G., R. Monshouwer, I. H. M. van Stokkum, R. van Grondelle, and H. van Amerongen. 1997b. Ultrafast singlet excitation transfer from carotenoids to chlorophylls via different pathways in light-harvesting complex II of higher plants. *Chem. Phys. Lett.* 264:279–284.

Peterman, E. J. G., T. Pullerits, R. van Grondelle, and H. van Amerongen. 1997c. Electron-phonon coupling and vibronic fine structure of light-harvesting complex II of green plants: temperature dependent absorption and high-resolution fluorescence spectroscopy. *J. Phys. Chem. B.* 101: 4448–4457.

Sauer, K., J. R. L. Smith, and A. J. Schultz. 1966. Dimerization of chlorophyll a, chlorophyll b and bacterial chlorophyll in solution. *J. Am. Chem. Soc.* 88:2681–2688.

Savikhin, S., H. van Amerongen, S. L. S. Kwa, R. van Grondelle, and W. S. Struve. 1994. Low-temperature energy transfer in LHC-II trimers from the Chl *a*/*b* light-harvesting antenna of photosystem II. *Biophys. J.* 66:1597–1603.

Shipmann, L. L., and D. L. Hausmann. 1979. Förster transfer rates for chlorophyll *a*. *Photochem. Photobiol.* 29:1163–1167.

Struve, W. S. 1995. Theory of electronic energy transfer. *In* Anoxygenic Photosynthetic Bacteria. R. E. Blankenship, M. T. Madigan, and C. E. Bauer, editors. Kluwer Academic Publishers, Dordrecht, the Netherlands. 297–313.

Trinkunas, G., J. P. Connelly, M. G. Müller, L. Valkunas, and A. R. Holzwarth. 1997. Model for the excitation dynamics in the light-harvesting complex II from higher plants. *J. Phys. Chem. B.* 101: 7313–7320.

van Amerongen, H., B. M. van Bolhuis, S. Betts, R. Mei, R. van Grondelle, C. F. Yocum, and J. P. Dekker. 1994. Polarized fluorescence and absorption of macroscopically aligned light harvesting complex II. *Biophys. J.* 67:227–234.

van der Vos, R., D. Carbonera, and A. J. Hoff. 1991. Microwave and optical spectroscopy of carotenoid triplets in light-harvesting complex LHC II of spinach by absorbance-detected magnetic resonance. *Appl. Magn. Reson.* 2:179–202.

van Grondelle, R., J. P. Dekker, T. Gillbro, and V. Sundström. 1994. Energy transfer in photosynthesis. *Biochim. Biophys. Acta.* 1187:1–65.

van Stokkum, I. H. M., T. Scherer, A. M. Brouwer, and J. W. Verhoeven. 1994. Conformational dynamics of flexibility and semirigidly bridged electron donor-acceptor systems as revealed by spectrotemporal parametrization of fluorescence. *J. Phys. Chem.* 98:852–866.

Visser, H. M., M.-L. Groot, F. van Mourik, I. H. M. van Stokkum, J. P. Dekker, and R. van Grondelle. 1995. Subpicosecond transient absorption difference spectroscopy on the reaction center of photosystem II: radical pair formation at 77 K. *J. Phys. Chem.* 99:15304–15309.

Visser, H. M., F. J. Kleima, I. H. M. van Stokkum, R. van Grondelle, and H. van Amerongen. 1996. Probing the many energy-transfer processes in the photosynthetic light-harvesting complex II at 77 K using energy-selective sub-picosecond transient absorption spectroscopy. *Chem. Phys.* 210:297–312.

Visser, H. M., F. J. Kleima, I. H. M. van Stokkum, R. van Grondelle, and H. van Amerongen. 1997. Probing the many energy-transfer processes in the photosynthetic light-harvesting complex II at 77 K using energy-selective sub-picosecond transient absorption spectroscopy. *Chem. Phys.* 215:299 (erratum).